Re-analysis of the $\Lambda(1520)$ photoproduction reaction

Ju-Jun Xie,[1, 2, 3, *] En Wang,[2, †] and J. Nieves[2, ‡]

[1]*Institute of Modern Physics, Chinese Academy of Sciences, Lanzhou 730000, China*
[2]*Instituto de Física Corpuscular (IFIC), Centro Mixto CSIC-Universidad de Valencia,*
Institutos de Investigación de Paterna, Aptd. 22085, E-46071 Valencia, Spain
[3]*State Key Laboratory of Theoretical Physics, Institute of Theoretical Physics,*
Chinese Academy of Sciences, Beijing 100190, China
(Dated: February 20, 2014)

Based on previous studies that support the important role of the $N^*(2120)D_{13}$ resonance in the $\gamma p \to K^+\Lambda(1520)$ reaction, we make a re-analysis of this $\Lambda(1520)$ photoproduction reaction taking into account the recent CLAS differential cross-section data. In addition to the contact, $t-$channel $\bar{K}$ exchange, $s-$channel nucleon pole and $N^*(2120)$ [previously called $N^*(2080)$] resonance contributions, which have been already considered in previous works, we also study the $u-$channel $\Lambda(1115)$ hyperon pole term. The latter mechanism has always been ignored in all theoretical analysis, which has mostly relied on the very forward K^+ angular LEPS data. It is shown that when the contributions from the $N^*(2120)$ resonance and the $\Lambda(1115)$ hyperon are taken into account, both the new CLAS and the previous LEPS data can be simultaneously described. We also show that the contribution from the $u-$channel $\Lambda(1115)$ pole term produces an enhancement for large K^+ angles, and it becomes more and more relevant as the photon energy increases, being essential to describe the CLAS differential cross sections at backward angles. Furthermore, we find that the new CLAS data also favor the existence of the $N^*(2120)$ resonance, and that these measurements can be used to further constrain its properties.

PACS numbers: 13.75.Cs.; 14.20.-c.; 13.60.Rj.

I. INTRODUCTION

The baryon spectrum and baryon couplings studied from experimental data are two of the most important issues in hadronic physics and they are attracting great attention (see Ref. [1] for a general review). Nucleon excited states below 2.0 GeV have been extensively studied, from both the experimental and the theoretical points of view [2]. Thus, there exists abundant information on most of their parameters, such as masses, total and partial decay widths, and decay modes. However, the current knowledge on the properties of states around or above 2.0 GeV is still in its infancy [2]. On the other hand, in this region of energies, many theoretical predicted *missing N^* states*, within the constituent quark [3] or chiral unitary [4–8] approaches, have so far not been observed. Because a large number of effective degrees of freedom will induce a great number of excited states, the *missing N^* states* problem seems to favor diquark configurations, which could lead to reduced numbers of degrees of freedom. Such schemes would naturally predict a smaller number of excited N^* states [9]. Thus, the study of the possible role played by the 2.0 GeV region nucleon resonances in the available new accurate data from the LEPS and CLAS Collaborations is timely and could shed light on the complicated dynamics that governs the highly excited nucleon (or in general baryon)

spectrum.

The associated strangeness production reaction $\gamma p \to K^+\Lambda(1520)$ might be adequate to study the N^* resonances around 2.0 GeV, as long as they have significant couplings to the $K\Lambda(1520)$ pair. This is because the $K\Lambda(1520)$ is a pure isospin $1/2$ channel and the threshold is about 2.0 GeV ($m_K + M_{\Lambda(1520)} \simeq 2.0$ GeV). Besides, this reaction requires the creation of an $\bar{s}s$ quark pair. Thus, a thorough and dedicated study of the strangeness production mechanism in this reaction has the potential to achieve a deeper understanding of the interaction among strange hadrons and, also, of the nature of the baryon resonances.

There were pioneering measurements at Cornell [10] and CEA [11], and in the 1970s, the first $\gamma p \to K^+\Lambda(1520)$ cross sections in the high-energy region $E_\gamma = 11$ GeV (SLAC [12]), and in the range 2.8-4.8 GeV (LAMP2 Collaboration [13]) were reported. In 2001, the CLAS Collaboration investigated this process in electroproduction [14], at electron beam energies of 4.05, 4.25, and 4.46 GeV, in the kinematic region spanning the squared momentum transfer Q^2 from 0.9 to 2.4 GeV^2, and for invariant masses from 1.95 to 2.65 GeV. Later, in 2010, this reaction was examined at photon energies below 2.4 GeV in the SPring-8 LEPS experiment using a forward-angle spectrometer and polarized photons [15, 16], and from threshold to 2.65 GeV with the SAPHIR detector at the electron stretcher facility ELSA in Bonn [17]. Very recently, the exclusive $\Lambda(1520)$ ($\equiv \Lambda^*$) photoproduction cross section has been measured by using the CLAS detector for energies from threshold up to an invariant γp mass $W = 2.85$ GeV [18].

The theoretical activity has run in parallel. There ex-

ist several effective hadron Lagrangian studies [19–25] exist for laboratory photon energies ranging from threshold up to about 5 GeV. These theoretical studies have traditionally been limited by the lack of knowledge on the $\bar{K}^* N \Lambda^*$ coupling strength. This fact, in conjunction with the use of largely different form factors to account for the compositeness of the hadrons, has led to contradicting predictions of the dominant reaction mechanism in the process. Some light was shed on this issue in [23]. There, the SU(6) Weinberg-Tomozawa chiral unitary model proposed in [26] was used to predict a relatively small $\bar{K}^* N \Lambda^*$ coupling and, hence, to conclude that the $\bar{K}$ exchange and contact mechanisms dominated the $\gamma p \to K^+ \Lambda(1520)$ reaction. Besides, in the higher energy region, the quark-gluon string mechanism with the $\bar{K}$ Regge trajectory was shown [23] to reproduce both the LAMP2 energy and the angular distribution data [13].

The theory groups have also paid attention to another distinctive feature of the data. The LEPS energy dependence of the forward-angle cross section rises from threshold to a maximum near $W = 2.15$ GeV, followed by a decline [16]. It was suggested that this could be an effect of the odd parity D_{13} (L_{2T2J}) N^* intermediate resonance at around 2.1 GeV [21, 24, 25, 27]. In the scheme of Refs. [21] and [27], the contribution of the spin-parity $J^P = 3/2^-$ $N^*(2080)$ $(\equiv N^*)$ resonance[1] turned out to be very small. Hence in these works, such a contribution was not expected to explain the bump structure at forward angles reported by LEPS. This was primarily owing to the unnecessarily small $N^* \Lambda^* K$ coupling and probably the excessively large width of the resonance used in these references. However in Ref. [24], within the effective Lagrangian approach of Ref. [23], the role played by the $N^*(2120)$ resonance in the $\gamma p \to K^+ \Lambda(1520)$ reaction was revisited, and found that the experimental LEPS Collaboration data could be fairly well described assuming a large $N^* \Lambda^* K$ coupling, which would be supported by some constituent quark models [29]. Yet, the recent analysis carried out in [30] taking the hadron resonance couplings from [29], shows that the D_{13} $N^*(2120)$ resonance also plays an important role in reproducing the $\Lambda(1520)$ electroproduction CLAS data [14] properly. A large $N^* \Lambda^* K$ coupling scenario has also been investigated in the $pp \to pK^+ \Lambda^*$ and $\pi^- p \to K^0 \Lambda^*$ hadronic $\Lambda(1520)$ production reactions [31]. Note that a resonance with these quantum numbers in the 2.1 GeV energy region, albeit with some uncertainty in the precise position, is unavoidable owing to the attractive character and strength of the vector-baryon interaction within the schemes of Refs. [4] and [6]. Furthermore, a recent

analysis [32] of the $\gamma p \to K^0 \Sigma^+$ CBELSA/TAPS data [33], which exhibits a peak in the cross section around $\sqrt{s} = 1.9$ GeV followed by a fast downfall around $\sqrt{s} = 2.0$ GeV, also provides support for the existence of a $J^P = 3/2^-$ nucleon excited state around 2 GeV.

On the other hand, the comparison of the recent CLAS measurements [18] with different effective Lagrangian model predictions [20, 25], obtained by using the parameters fitted to the LEPS [15, 16] and LAMP2 [13] data, indicates that the current model calculations can not describe the CLAS differential cross sections well over the entire energy and angular ranges available in the experiment.

In the present work, we aim to achieve an improved description of the recent CLAS data, which would provide further support for the existence of the $N^*(2120)$ resonance, and additional constraints on its properties. Within the scheme of Ref. [24], and in addition to the contact, $t-$channel $\bar{K}$ exchange, and $s-$channel nucleon and $N^*(2120)$ resonance pole contributions, we also study the $u-$channel $\Lambda(1115)$ $(\equiv \Lambda)$ hyperon pole term. The latter mechanism has been ignored in all previous calculations [20, 23–25] because information on the $\Lambda\Lambda\gamma$ coupling is scarce [22], and because it is expected to provide small contributions for forward K^+ angles, where the LEPS data lie. However, $u-$channel mechanisms might make important contributions at the backward K^+ angles that have become accessible in the recent CLAS experiment. As a consequence, it is not surprising, that previous theoretical calculations that reasonably described the LEPS data, were not as successful in describing the recent CLAS differential cross sections, which span a much wider range of K^+ angles.

Taking these considerations into account, and using the combination of the effective Lagrangian approach and the isobar model, we present in this work a combined theoretical analysis of the recent $\gamma p \to K^+ \Lambda(1520)$ CLAS [18] and LEPS [16] data that includes the contribution from the $u-$channel Λ hyperon pole term.

The paper is organized as follows. In Sec. II, we discuss the formalism and the main ingredients of the model, while our numerical results and discussion are presented in Sec. III. Finally, a short summary and conclusions are given in Sec. IV.

II. FORMALISM AND INGREDIENTS

The invariant scattering amplitudes that enter our model for calculation of the total and differential cross sections for the reaction[2]

$$\gamma(k_1, \lambda) p(k_2, s_p) \to K^+(p_1) \Lambda^*(p_2, s_{\Lambda^*}) \qquad (1)$$

---

[1] Before the 2012 Particle Date Group (PDG) review, all the evidence for a $J^P = 3/2^-$ state with a mass above 1.8 GeV was filed under a two-star $N^*(2080)$. There is now evidence [28] of two states in this region, and the PDG has split the older data (according to mass) between a three-star $N^*(1875)$ and a two-star $N^*(2120)$ [2].

[2] The definition of the kinematical and polarization variables is the same as in Ref. [24] [see also Eq. (1) and Figs. 1 and 2].
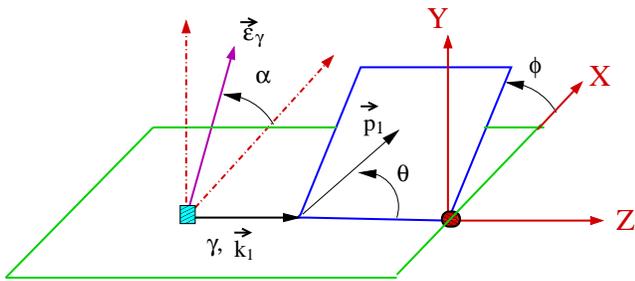
FIG. 1: (Color online) Definition of the different angles used in this work.

are defined as

$$-iT_i = \bar{u}_\mu(p_2, s_{\Lambda^*}) A_i^{\mu\nu} u(k_2, s_p)\epsilon_\nu(k_1, \lambda) \qquad (2)$$

where u_μ and u are dimensionless Rarita-Schwinger and Dirac spinors, respectively, while $\epsilon_\nu(k_1, \lambda)$ is the photon polarization vector. In addition, s_p and s_{Λ^*} are the baryon polarization variables. The sub-index i stands for the contact, $t-$channel antikaon exchange, $s-$channel nucleon and N^* pole terms (depicted in Fig. 1 of Ref. [24]) and novel $u-$channel Λ pole mechanism. In our final results, and for simplicity, we do not consider the $u-$channel $\Sigma^0(1193)$ pole term, as we expect its contribution to be much smaller than that from the $\Lambda(1115)$ hyperon. We come back to this point below. Moreover, higher-excited hyperons would be farther off-shell in the $u-$channel, and have not been taken into account either.

The explicit expressions for the reduced $A_i^{\mu\nu}$ amplitudes of the first four mechanisms, Fig. 1 of Ref. [24], can be found in that reference. Here, we only give details on the $u-$channel Λ pole amplitude, $A_u^{\mu\nu}$, associated with the diagram in Fig. 2. It is obtained from the effective interaction Lagrangian densities,

$$\mathcal{L}_{\gamma\Lambda\Lambda^*} = -\frac{ih_1}{2m_\Lambda}\bar{\Lambda}_\mu^*\gamma_\nu F^{\mu\nu}\Lambda$$
$$+\frac{h_2}{(2m_\Lambda)^2}\bar{\Lambda}_\mu^* F^{\mu\nu}\partial_\nu\Lambda + \text{h.c.} \qquad (3)$$

$$\mathcal{L}_{KN\Lambda} = -ig_{KN\Lambda}\bar{\Lambda}\gamma_5 K^- p + \text{h.c.}, \qquad (4)$$

Note that the $\gamma\Lambda\Lambda^*$ vertex is gauge invariant by itself, as A_μ and $F_{\mu\nu} = (\partial_\mu A_\nu - \partial_\nu A_\mu)$ are the photon field and electromagnetic-field tensors, respectively. h_1 and h_2 are magnetic coupling constants, while $g_{KN\Lambda}$ is a strong one. We take $g_{KN\Lambda} \sim -14$ as estimated from the SU(3) flavor symmetry [34] Bonn-Jülich model for the meson-exchange hyperon-nucleon interactions in free scattering [35]. Note that at lowest order in the chiral expansion [36, 37],

$$\frac{g_{\pi^0 pp}}{g_{K^+ p\Lambda}} \sim -\frac{D+F}{\frac{D+3F}{\sqrt{3}}}, \qquad \frac{g_{K^+ p\Sigma^0}}{g_{K^+ p\Lambda}} \sim -\frac{D-F}{\frac{D+3F}{\sqrt{3}}}, \qquad (5)$$

with $D \sim 0.8$ and $F \sim 0.5$, which justifies $|g_{KN\Lambda}/g_{\pi NN}| \sim 1$. Besides, we see that the $g_{K^+ p\Sigma^0}$ is

about four or five times smaller than $g_{K^+ p\Lambda}$, and this is also compatible with the findings in [35]. The latter relationship between couplings gives support for neglecting the $u-$channel Σ^0 pole contribution, despite that the strength of the electromagnetic $\gamma\Sigma^0\Lambda^*$ coupling could be similar to, or even larger than, that involving the $\Lambda(1115)$ hyperon [38]. The Σ^0 radiative decay of the $\Lambda(1520)$ has
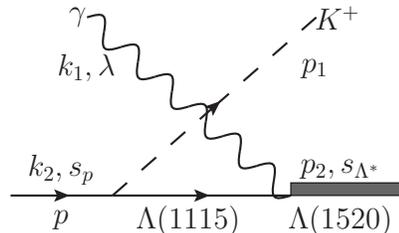

FIG. 2: The $u-$channel Λ pole mechanism. In the diagram, we also show the definition of the kinematical (k_1, k_2, p_1, p_2) and polarization $(\lambda, s_p, s_{\Lambda^*})$ variables that we use in the present calculation. In addition, we use $q_u = k_2 - p_1 = p_2 - k_1$, with $u = q_u^2$.

not been observed yet, while $\Gamma(\Lambda(1520) \to \Lambda\gamma)$ has been measured to be of the order of 130 keV [2]. There exist various (Table I) theoretical estimates [39–46] for the $\Gamma(\Lambda(1520) \to \Sigma^0\gamma)$ width, ranging from the 17 keV predicted within the MIT bag model [40] up to the 293 keV obtained in the RCQM (relativistic constituent quark model) approach followed in [41]. If the $\Lambda(1520)$ were a SU(3) singlet and assuming that the photon is a $U-$spin singlet, $U-$spin invariance guarantees that decay into the $U-$spin triplet linear combination $(\Sigma^0 + 3\Lambda)$ would be 0 [38]. Thus one would predict[3] $\Gamma(\Lambda(1520) \to \Sigma^0\gamma) \sim 3\times$ (phase space) $\times\Gamma(\Lambda(1520) \to \Lambda\gamma) \sim 230$ keV, in the upper-band of the various predictions listed in Table I.

Despite this large ambiguity, one can safely conclude that even though the electromagnetic $\gamma\Sigma^0\Lambda^*$ coupling was bigger than the $\gamma\Lambda\Lambda^*$ one, it would not be large enough to compensate for the big reduction induced by the ratio of hadronic couplings $\left(g_{K^+ p\Sigma^0}/g_{K^+ p\Lambda}\right)^2 \sim 1/20$. Hence, it seems reasonable to assume that the $\Sigma^0(1193)$ contribution to the $\gamma p \to K^+\Lambda(1520)$ reaction would be much smaller than that of the $\Lambda(1115)$ hyperon. On the other hand, taking into account the $u-$channel $\Sigma^0(1193)$ term would require adopting some theoretical model for the electromagnetic $\Lambda^*\Sigma^0\gamma$ amplitude. However, we see that important discrepancies among the various approaches, even in predicting the radiative decay width $\Gamma(\Lambda(1520) \to \Sigma^0\gamma)$. Fitting this amplitude to data

---

[3] In the original work in Ref. [38], it was assumed that the phase space scaled as the decaying photon momentum from what follows $\Gamma(\Lambda(1520) \to \Sigma^0\gamma) \sim 2.5\times\Gamma(\Lambda(1520) \to \Lambda\gamma)$ [38]. However, as we see below (Eqs. (8)–(10)), the decay width rather scales down as the cube of the photon momentum, which leads to the lower value, about 230 keV.

TABLE I: Theoretical predictions (in keV) for the radiative width $\Gamma(\Lambda(1520) \to \Sigma^0\gamma)$.

Approach	NRQM	MIT Bag	RCQM	Chiral Bag	Algebraic	BonnBSCQM	χQM	UChPT
Ref.	[39, 40]	[40]	[41]	[42]	[43]	[44]	[45]	[46]
Γ [keV]	55–75	17	293	49	180	157	92	71

is not a realistic option either, because both the Λ and the Σ^0 $u-$channel poles are quite close, and the available data cannot effectively discriminate between their contributions. Thus, in the final results, and for the sake of simplicity, we do not include the $u-$channel $\Sigma^0(1193)$ mechanism. Nevertheless, we estimate the possible impact of this term assuming $U-$spin SU(3) symmetry.

With the above Lagrangians, one readily finds

$$A_u^{\mu\nu} = \left(\frac{h_1}{2m_\Lambda}(k_1^\mu\gamma^\nu - g^{\mu\nu}\slashed{k}_1) + \frac{h_2}{(2m_\Lambda)^2}(k_1^\mu q_u^\nu - g^{\mu\nu}k_1\cdot q_u)\right)$$
$$\times \frac{\slashed{q}_u + m_\Lambda}{u - m_\Lambda^2}g_{KN\Lambda}\gamma_5 f_u, \qquad (6)$$

where m_Λ and q_u are the mass and the four-momentum of the $\Lambda(1115)$, respectively, and $u = q_u^2$. In addition, we should introduce in the above equation the compositeness of the hadrons. This has been achieved by including the form factor f_u in the amplitude of Eq. (6),

$$f_u = \frac{\Lambda_u^4}{\Lambda_u^4 + (u - m_\Lambda^2)^2}, \qquad (7)$$

whose form is similar to those used in [24] to construct the form-factors that appear in the rest of the amplitudes in the model. In principle, the cut off Λ_u is a free parameter of the model, but in practice we will fix it to a common value taken by Λ_t and Λ_s as well.[4]

The $\gamma\Lambda\Lambda^*$ coupling constants h_1 and h_2 could be fixed from the $\Lambda^* \to \Lambda\gamma$ partial decay width [2],

$$\Gamma_\gamma = \frac{m_\Lambda k_\gamma^2}{2\pi M_{\Lambda^*}}\left(|A_{1/2}|^2 + |A_{3/2}|^2\right), \qquad (8)$$

with,

$$A_{1/2} = \frac{\sqrt{6}}{12}\sqrt{\frac{k_\gamma}{m_\Lambda M_{\Lambda^*}}}\left(h_1 + \frac{M_{\Lambda^*}h_2}{4m_\Lambda^2}(M_{\Lambda^*} + m_\Lambda)\right) \quad (9)$$

$$A_{3/2} = \frac{\sqrt{2}}{4m_\Lambda}\sqrt{\frac{k_\gamma M_{\Lambda^*}}{m_\Lambda}}\left(h_1 + \frac{h_2}{4m_\Lambda}(M_{\Lambda^*} + m_\Lambda)\right), (10)$$

where $k_\gamma = (M_{\Lambda^*}^2 - m_\Lambda^2)/(2M_{\Lambda^*})$ is the photon center of mass (c.m.) frame decay momentum. With the value of

$\Gamma_\gamma = 0.133$ MeV, as quoted in the PDG [2], we could get a constraint on the values of h_1 and h_2,

$$ah_1^2 + bh_2^2 + ch_1h_2 = d, \qquad (11)$$

with

$$a = \frac{m_\Lambda^2 + 3M_{\Lambda^*}^2}{24m_\Lambda^3 M_{\Lambda^*}}k_\gamma^3, \qquad b = \frac{M_{\Lambda^*}(m_\Lambda + M_{\Lambda^*})^2}{96m_\Lambda^5}k_\gamma^3, (12)$$

$$c = \frac{(m_\Lambda + M_{\Lambda^*})(m_\Lambda + 3M_{\Lambda^*})}{48m_\Lambda^4}k_\gamma^3, \quad d = \frac{2\pi M_{\Lambda^*}\Gamma_\gamma}{m_\Lambda} (13)$$

With the ingredients given above, the unpolarized c.m. differential cross section can be easily obtained as,

$$\frac{d\sigma}{d(\cos\theta_{\text{c.m.}})} = \frac{|\vec{k}_1^{\text{c.m.}}||\vec{p}_1^{\text{c.m.}}|}{4\pi}\frac{M_N M_{\Lambda^*}}{(W^2 - M_N^2)^2}$$
$$\times \sum_{s_p, s_{\Lambda^*}, \lambda}|T|^2 \qquad (14)$$

with W the invariant mass of the γp pair. Further, $\vec{k}_1^{\text{c.m.}}$ and $\vec{p}_1^{\text{c.m.}}$ are the photon and K^+ meson c.m. three-momenta, and $\theta_{\text{c.m.}}$ is the K^+ polar scattering angle (Fig. 1). The differential cross section $d\sigma/d(\cos\theta_{\text{c.m.}})$ depends on W and also on $\cos\theta_{\text{c.m.}}$.

As mentioned above, the model accounts for a total of five mechanisms: contact, $t-$channel antikaon exchange, $s-$channel nucleon and N^* pole terms, evaluated in [24], and the $u-$channel Λ pole contribution discussed here. In principle, the free parameters of the model are: (i) the mass and width (M_{N^*} and Γ_{N^*}) of the $N^*(2120)$ resonance, (ii) the cut off parameters $\Lambda_s = \Lambda_t = \Lambda_u \equiv \Lambda_B$ and Λ_R, and (iii) the $N^*(2120)$ resonance electromagnetic γNN^* (ef_1, ef_2) and strong $N^*\Lambda^*K$ (g_1, g_2) couplings and the $\Lambda(1520)$ magnetic $\gamma\Lambda\Lambda^*$ (h_1) one. Note that the second coupling h_2 in Eq. (4) is given in terms of h_1 and the Λ^* radiative decay width (see Eq. (11)).

In the next section, we fit the parameters of the model to the differential cross-section data from the CLAS and LEPS Collaborations.

III. NUMERICAL RESULTS AND DISCUSSION

First, we have performed[5] a nine-parameter ($ef_1, ef_2, g_1, g_2, \Lambda_s = \Lambda_t = \Lambda_u \equiv \Lambda_B, \Lambda_R, M_{N^*}, \Gamma_{N^*}$ and h_1)

---

[4] These are other cut offs that enter into the form factors that we include in the $t-$channel antikaon exchange, $s-$channel nucleon pole and contact amplitudes [24].

[5] We take $M_{\Lambda^*} = 1.5195$ GeV, $m_K = 0.4937$ GeV and $m_\Lambda = 1.1157$ GeV.

TABLE II: Values of some parameters determined in this work and in Ref. [24]. Fit I (II) parameters have been adjusted to the CLAS (combined CLAS [18] and LEPS [16]) $\gamma p \to K^+ \Lambda(1520)$ $d\sigma/d(\cos\theta_{\text{c.m.}})$ data, while fit C in Ref. [24] was obtained by considering only the LEPS differential cross sections. LEPS data lie in the K^+ forward angle region and were taken below $E_\gamma = 2.4$ GeV, while the recent CLAS measurements span a much larger K^+ angular and photon energy regions. Finally, we also list for each fit the predicted $N^*(2120)$ width $\Gamma_{N^*\to\Lambda^*K}$, helicity amplitudes for the positive-charge state and the h_2 electromagnetic $\gamma\Lambda\Lambda^*$ coupling.

	Fitted Parameters		
	This work		Ref. [24]
	Fit I	Fit II	Fit C
g_1	1.7 ± 0.4	1.6 ± 0.2	1.4 ± 0.3
g_2	4.6 ± 1.2	2.2 ± 0.5	5.5 ± 1.8
Λ_B [MeV]	630 ± 2	620 ± 2	604 ± 2
Λ_R [MeV]	933 ± 52	1154 ± 47	909 ± 55
ef_1	0.123 ± 0.015	0.126 ± 0.012	0.177 ± 0.023
ef_2	-0.094 ± 0.014	-0.097 ± 0.010	-0.082 ± 0.023
M_{N^*} [MeV]	2172 ± 10	2135 ± 4	2115 ± 8
Γ_{N^*} [MeV]	287 ± 54	184 ± 11	254 ± 24
h_1	0.68 ± 0.05	0.64 ± 0.05	–
χ^2/dof	2.5	2.5	1.2
χ^2/dof (without N^*)	5.6	9.9	24
χ^2/dof (without Λ)	3.0	3.0	–
χ^2/dof (without N^* and Λ)	6.3	9.9	–
	Derived Observables		
$A_{1/2}^{p^*}[10^{-3}\text{GeV}^{-1/2}]$	-7.6 ± 3.9	-7.3 ± 3.0	3.6 ± 8.6
$A_{3/2}^{p^*}[10^{-2}\text{GeV}^{-1/2}]$	2.5 ± 1.0	2.5 ± 0.8	5.8 ± 2.1
$\Gamma_{N^*\to\Lambda^*K}$ [MeV]	56 ± 27	30 ± 8	19 ± 7
$\frac{\Gamma_{N^*\to\Lambda^*K}}{\Gamma_{N^*}}[\%]$	19.0 ± 10.3	16.2 ± 4.2	7.5 ± 2.8
h_2	-0.43 ± 0.08	-0.38 ± 0.07	–

χ^2−fit to the $d\sigma/d(\cos\theta_{\text{c.m.}})$ data from the CLAS Collaboration [18] (fit I). There is a total of 157 available data points displayed in Fig. 3. The $d\sigma/d(\cos\theta_{\text{c.m.}})$ data, as a function of $\cos\theta_{\text{c.m.}}$, are given for nine intervals of the invariant γp mass W from the reaction threshold 2.02 GeV up to 2.85 GeV. To compute the cross sections in each interval we always use the corresponding mean value of W. (We have checked that variations with respect to calculation of the average value of the differential cross sections for each W range turn out to be very small.) We have also carried out a combined fit to the CLAS [18] and LEPS [16], $d\sigma/d(\cos\theta_{\text{c.m.}})$ data (fit II). In this second fit, we have a total of 216 data points (in addition to the former CLAS differential cross sections, we have also fitted to the LEPS data depicted in Fig. 4).

The fitted parameters from the above two fits are listed in Table II, where we also report our previous results from a best fit (fit C of Ref. [24]) only to the LEPS data of Ref. [16]. We also give for each fit, the predicted nucleon D_{13} resonance width $\Gamma_{N^*\to\Lambda^*K}$ (Eq. (18) in Ref. [24]), helicity amplitudes (Eqs. (15) and (16) in Ref. [24]) for the positive-charge state and the h_2 magnetic $\gamma\Lambda\Lambda^*$ cou-

pling [Eq. (11)].[6]

As commented before, LEPS data lie in the K^+ forward angle region and were taken below $E_\gamma = 2.4$ GeV, while the recent CLAS measurements span a much larger K^+ angular and photon energy regions. The χ^2/dof for both fit I and fit II are acceptable, of the order of 2.5. The new CLAS measurements are quite accurate (excluding some data close to threshold) with statistical errors ranging from about 10%, at high scattering angles, down to 5% or less for forward angles. The systematical errors of the experimental data (11.6% [18] and 5.92% [16], for CLAS and LEPS, respectively) have been added in quadratures to the statistical ones and taken into account in the present new fits. We see that the N^* resonance parameters from the new fits I and II turn out to be in reasonable agreement with those obtained in Ref. [24]. Thus, the first conclusion is that the CLAS data provide

---

[6] This is a second rank equation and it has two possible solutions. One of them turns out to be strongly disfavored by the χ^2−fit. To be more quantitative, in our final results (fit II), χ^2/dof would pass from 2.5 to 3.1 if the other solution were considered.

further support for the existence of an odd parity 3/2 wide nucleon resonance with a mass in the region of 2.1 GeV and a width of around 200 MeV. This is compatible with the Breit-Wigner parameters, $M_{BW} = 2.15 \pm 0.06$ GeV and $\Gamma_{BW} = 330 \pm 45$ MeV, reported in [28]. The latter reference also provides experimental values for its helicity amplitudes

$$A^{p^*}_{1/2}[10^{-3}\text{GeV}^{-1/2}] \; = \; 125 \pm 45 \qquad (15)$$

$$A^{p^*}_{3/2}[10^{-2}\text{GeV}^{-1/2}] \; = \; 15 \pm 6 \,, \qquad (16)$$

which however do not seem entirely consistent with previous measurements [47]

$$A^{p^*}_{1/2}[10^{-3}\text{GeV}^{-1/2}] \; = \; -20 \pm 8 \qquad (17)$$

$$A^{p^*}_{3/2}[10^{-2}\text{GeV}^{-1/2}] \; = \; 1.7 \pm 1.1 \qquad (18)$$

quoted in the 2008 PDG edition [48], which in turn are in better agreement with our predictions in Table II. Note that the latter helicity amplitudes are used in [30], where the $ep \to eK^+\Lambda(1520)$ CLAS data in Ref. [14] were successfully described. Nevertheless, given the two-star status (evidence of existence is only fair) granted to the $N^*(2120)$ resonance in the multichannel partial wave analysis of pion and photo-induced reactions off protons carried out in [28], the discrepancy with our predicted helicity amplitudes should not be used to rule out our fits, but rather one could use them to further constrain these elusive observables. On the other hand, within this scheme, the $N^*(2120)$ resonance would have a large partial decay width into Λ^*K, which is compatible with the findings of the constituent quark model approach in Ref. [29]. Indeed, in that reference, $\Gamma_{N^*\to\Lambda^*K}$ is predicted to be 7^{+24}_{-6} MeV for a resonance mass of 2080 MeV. This value for the width is compatible within errors with the value of 30 ± 8 MeV found in this work. Moreover, because the $\Lambda(1520)K^+$ threshold is located so close to $M_{N^*} = 2080$ MeV, the width would increase by at least a factor of two if the resonance mass was instead taken as 2120 MeV. Hence, the constituent quark model of Ref. [29] would predict central values for $\Gamma_{N^*\to\Lambda^*K}$ in the vicinity of 15 MeV for the current PDG value of M_{N^*}. On the other hand, the width quoted in [29] leads to[7] $|g_1| = 1.25$, in good agreement with our fitted value. The analysis carried out in [30] for the $\Lambda(1520)$ electro-production reaction off the proton uses this value for g_1, fixes g_2 to 0 and, as mentioned above, uses the helicity amplitudes given in [47]. Thus, the set of N^* couplings used in [30], where the important role played by the D_{13} $N^*(2120)$ resonance is also highlighted, turns out to be similar to that found in this work.

The differential $d\sigma/d(\cos\theta_{\text{c.m.}})$ distributions from the combined fit (fit II) to the CLAS [18] and LEPS [16]

data are shown in Figs. 3 and 4, and compared with the experimental data. Only statistical errors are displayed in these two figures. The contributions from different mechanisms of the model are shown separately.

In the first of these two figures, the differential cross sections as a function of $\cos\theta_{\text{c.m.}}$, for different γp invariant mass intervals, are displayed and contrasted with the recent CLAS measurements. Near threshold the CLAS cross section is fairly flat. In the highest energy bin the cross section is quite forward peaked, with a hint of plateauing toward the most forward angles. Also evident is that the cross section flattens or even rises slightly toward large angles. We find an overall good description of the data, both at forward and at backward K^+ angles and for the whole range of measured γp invariant masses, W. We see that as W increases, the contribution of the $u-$channel $\Lambda(1115)$ pole term produces an enhancement at backward angles, and it becomes more and more relevant. Indeed, it turns out to be essential above $W \geq 2.35$ GeV and $\cos\theta_{\text{c.m.}} \leq -0.5$. The present model provides a better description of the recent CLAS data than that obtained within the schemes of Refs. [27] and [25], whose predictions are reported in [18]. The major improvement can be appreciated at backward angles, as it is mostly attributable to the $u-$channel $\Lambda(1115)$ pole mechanism.

For comparison, we also display in Fig. 3 the contribution from the $u-$channel $\Sigma^0(1193)$ term, which is not included in fit II. The $\Sigma^0(1193)$ amplitude takes the same form as that of the $\Lambda(1115)$ mechanism (Eq. (6)), with the obvious replacements of coupling constants and hyperon masses. For the electromagnetic ones, we have assumed $U-$spin invariance ($h^{\Sigma}_{1,2} = -\sqrt{3}h_{1,2}$), while we have taken $g_{K^+p\Sigma^0} = 3.2$, as deduced from leading order vector chiral symmetry (Eq. (5)). As anticipated, the $u-$channel Σ^0 contribution turns out to be a small fraction of the Λ one, and can be safely neglected.

In Fig. 4, the differential cross section deduced from the results of the nine-parameter fit II, as a function of the LAB frame photon energy and for different forward c.m. K^+ angles, is shown and compared both to CLAS [18] and to LEPS [16] data. In this figure, dashed (blue) and dotted (green) lines show the contributions from the background[8] and N^* resonance terms, respectively, while the solid (red) lines display the full result. We see that the bump structure in the differential cross section at forward K^+ angles is fairly well described thanks to the significant contribution from the N^* resonance in the $s-$channel. Indeed, these results are similar to those already reported and discussed in Ref. [24], and the description of these forward LEPS data achieved here is also comparable to that exhibited in Ref. [24]. The CLAS data points shown in Fig. 4 were obtained from the appropriate CLAS cross sections displayed in Fig. 3,

---

[7] The width is rather insensitive to g_2 because its contribution is suppressed by the K^+ meson c.m. three-momentum.

[8] The contribution of the $u-$channel $\Lambda(1115)$ pole mechanism for these forward angles is negligible.
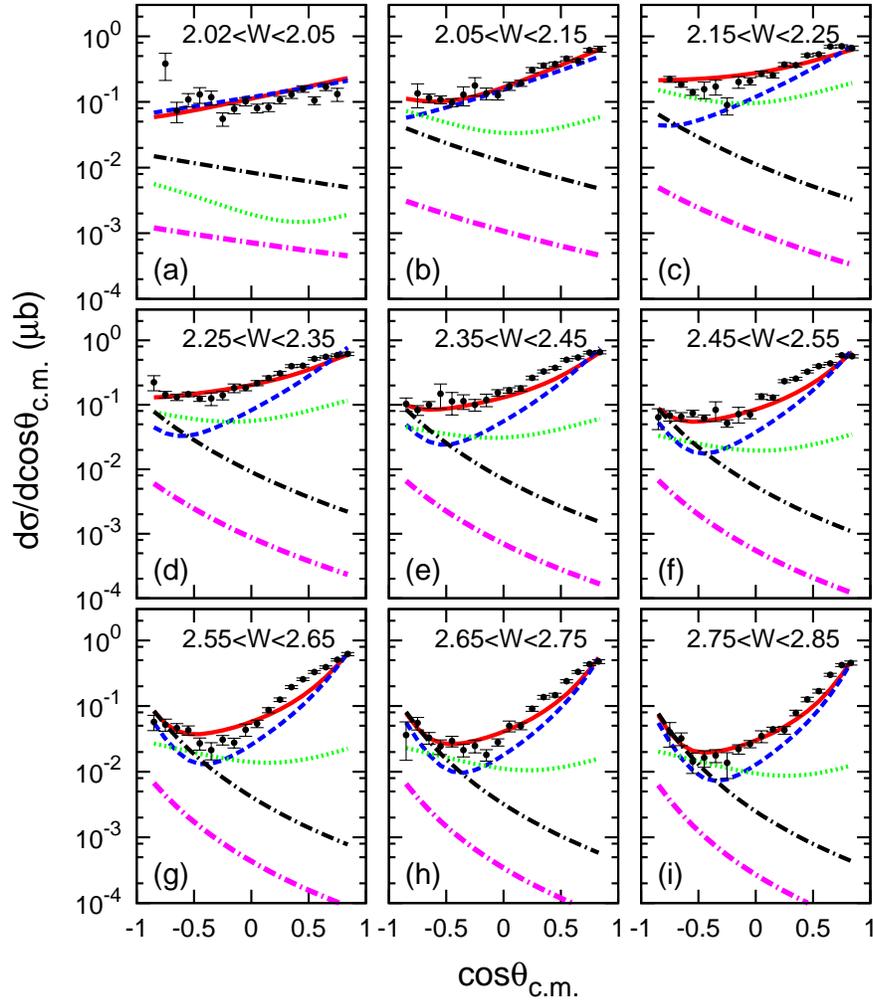
FIG. 3: (Color online) Fit II $\gamma p \to K^+ \Lambda(1520)$ differential cross sections as a function of $\cos \theta_{\text{c.m.}}$ compared with the CLAS data [18] for different γp-invariant mass intervals (in GeV). Only statistical errors are displayed. Dashed (blue) and dotted (green) lines show the contributions from background (contact, $t-$channel $\bar{K}$ exchange and $s-$channel nucleon and $u-$channel Λ pole mechanisms) and $N^*(2120)$ resonance terms, respectively. The Dash-dotted (black) curves represent for the $u-$channel $\Lambda(1115)$ contribution separately, while the solid (red) lines display the results obtained from the full model (background+N^*). Finally, the dash-dotted (magenta) curves represent the $u-$channel $\Sigma^0(1193)$ contribution, not included in the final results [solid (red) lines], as determined from electromagnetic $U-$spin ($h_{1,2}^\Sigma = -\sqrt{3}h_{1,2}$) and leading order chiral [Eq. (5)] symmetries.

relating W to the LAB photon energy. Returning to the latter figure, we see that our model underestimates the CLAS data for values of $\cos \theta_{\text{c.m.}}$ in the 0.5-0.75 interval, and in particular at high energies, $W \geq 2.3$ GeV. These discrepancies also show up in Figs. 4(a) and 4(b), where we can also appreciate that CLAS and LEPS data are only marginally consistent. However, one should bear in mind that systematic errors are not displayed in these plots, and they will make these differences less meaningful.

We have also performed several best fits, where either one or both of the $s-$channel $N^*(2120)$ resonance and the $u-$channel $\Lambda(1115)$ pole terms have been switched off. The corresponding χ^2/dof are also compiled in Table II, which turn out to be larger, and in most cases, unacceptable on statistical grounds.[9]

---

[9] Note that the quantitative effect on χ^2/dof of disconnecting the $u-$channel $\Lambda(1115)$ contribution is not big. This is because the forward angle LEPS data are rather insensitive to this mechanism, as well as the low energy CLAS cross section. As commented in the discussion of Fig. 3, only the backward high energy CLAS cross sections are being effected by this term, but there the qualitative effect is important. Despite the limited number of data points, which in addition suffer from large statistical fluc-
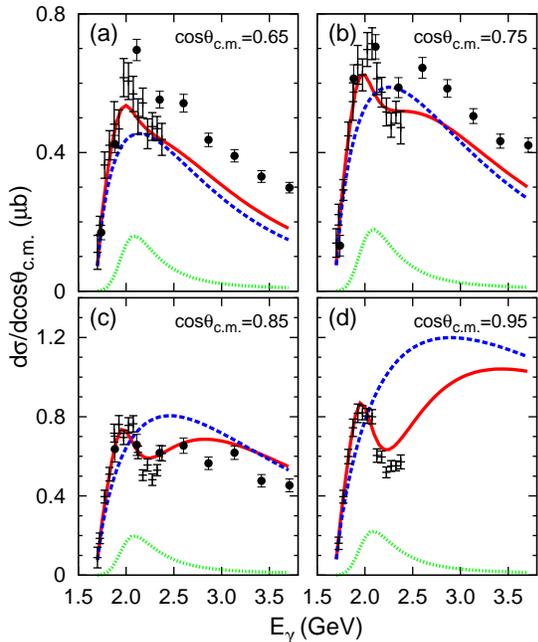
FIG. 4: (Color online) Fit II $\gamma p \rightarrow K^+\Lambda(1520)$ differential cross section as a function of the LAB frame photon energy for different c.m. K^+ polar angles. We also show the experimental LEPS [16] (crosses) and CLAS [18] (filled circles) data. Only statistical errors are displayed. Dashed (blue) and dotted (green) lines show the contributions from the background and $N^*(2120)$ resonance terms, respectively, while the red-solid lines represent the results obtained from the full model.
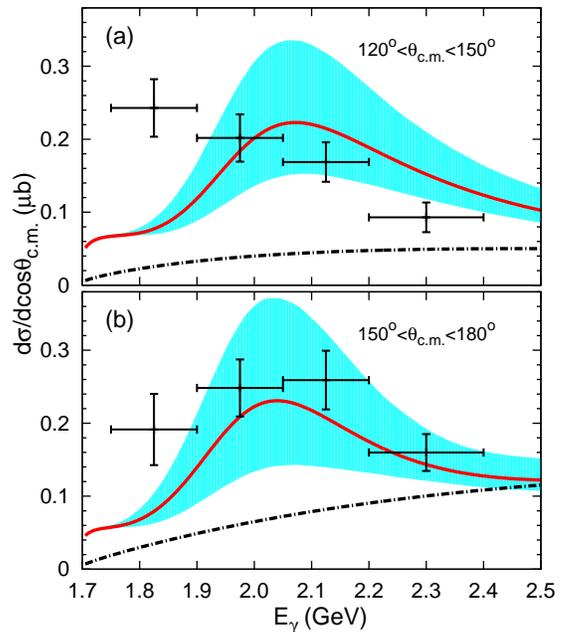
FIG. 5: (Color online) Fit II $\gamma p \rightarrow K^+\Lambda(1520)$ differential cross section as a function of the LAB frame photon energy for backward K^+ angles [solid (red) lines]. We display the average $\langle d\sigma/d(\cos\theta_{\mathrm{c.m.}})\rangle$ distribution (Eq. (19)) from the full model and compare it with LEPS data from Ref. [15]. (a, b) The 68% CL bands inherited from the Gaussian correlated statistical errors of the fit II parameters. Finally, the dash-dotted (black) curves show the $u-$channel $\Lambda(1115)$ contribution.

In Fig. 5, we compare the fit II predicted differential cross sections for large K^+ angles with the experimental data from Ref. [15]. There, events were accumulated for two angular intervals $\theta_{\mathrm{c.m.}} = (120-150)^0$ and $\theta_{\mathrm{c.m.}} = (150-180)^0$, with the photon energy varying in the region $1.9 \leq E_\gamma \leq 2.4$ GeV. Since the angular intervals are quite wide, we have partially integrated the differential cross section, and evaluated

$$\left\langle \frac{d\sigma}{d(\cos\theta_{\mathrm{c.m.}})} \right\rangle = \frac{\int_{\cos\theta_{\mathrm{c.m.}}^{\mathrm{up}}}^{\cos\theta_{\mathrm{c.m.}}^{\mathrm{dw}}} \frac{d\sigma}{d(\cos\theta_{\mathrm{c.m.}})} d(\cos\theta_{\mathrm{c.m.}})}{\int_{\cos\theta_{\mathrm{c.m.}}^{\mathrm{up}}}^{\cos\theta_{\mathrm{c.m.}}^{\mathrm{dw}}} d(\cos\theta_{\mathrm{c.m.}})}, \quad (19)$$

taking $(\theta_{\mathrm{c.m.}}^{\mathrm{dw}}, \theta_{\mathrm{c.m.}}^{\mathrm{up}})$ to be $(120^0, 150^0)$ or $(150^0, 180^0)$, respectively. In Fig. 5, the shaded regions account for the uncertainties inherited from those affecting the parameters compiled in Table II. They represent 68% confidence-level (CL) bands and were obtained using a Monte Carlo simulation. As shown in Figs. 5(a) and 5(b), the present model provides a fair description of these backward K^+ angular data. This is in sharp contrast to the results of

our previous work [24] (see Fig. 4 in Ref. [24]), where the $u-$channel $\Lambda(1115)$ mechanism was not considered. Indeed, the latter contribution is also depicted in Fig. 5. We see that it increases with the photon energy and that becomes quite relevant for the most backward angles [Fig. 5(b)].

Finally, we have also calculated the total cross section of the $\gamma p \rightarrow K^+\Lambda(1520)$ reaction as a function of the photon energy. The results are shown in Fig. 6 and compared to the experimental data from CLAS. We see that the model provides an excellent description of the integrated CLAS cross sections thanks to an important contribution from the photo-excitation of the $N^*(2120)$ resonance and its subsequent decay into a $\Lambda(1520)K^+$ pair. This mechanism seemed also to be responsible for the bump structure in the LEPS differential cross section at forward K^+ angles discussed in Fig. 4. Thus, one can definitely take advantage of the apparently important role played by this resonant mechanism in the LEPS and CLAS data to better constrain some of the $N^*(2120)$ properties (Table II), starting from its mere existence.

It is noteworthy that the contribution from the $u-$channel $\Lambda(1115)$ mechanism is very small in the inte-

---

tuations, the improvement on the total χ^2/dof is still significant (3.0 vs 2.5).
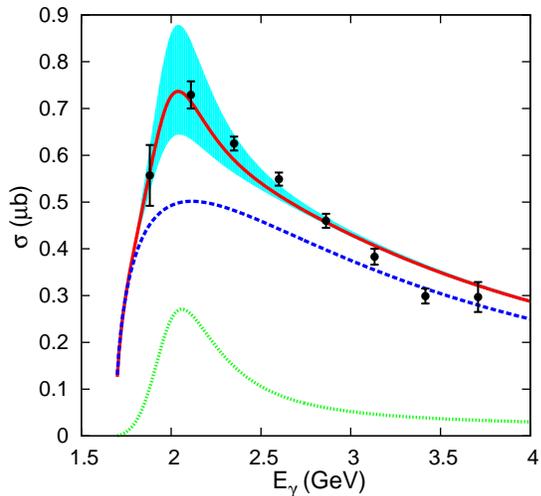
FIG. 6: (Color online) Total $\gamma p \to K^+ \Lambda^*$ cross section deduced from the results of fit II. We display it as a function of the LAB photon energy and compare with the CLAS data from Ref. [18]. Dashed (blue) and dotted (green) lines show the contributions from the background and N^* resonance terms, respectively, while the solid (red) line displays the results from the full model. The shaded region accounts for the 68% CL band inherited from the Gaussian correlated statistical errors of the fit II parameters.

grated cross section, as it is only significant for backward K^+ angles.

IV. SUMMARY AND CONCLUSIONS

We have carried out a new analysis of the $\gamma p \to \Lambda(1520)K^+$ reaction at low energies within an effective Lagrangian approach and the isobar model. We have presented results from a combined fit to the recent CLAS [18] and LEPS [16], $d\sigma/d(\cos\theta_{c.m.})$ data. Within the scheme of Ref. [24], and in addition to the contact, t−channel $\bar{K}$ exchange, and s−channel nucleon and $N^*(2120)$ resonance pole contributions, we have also studied the u−channel $\Lambda(1115)$ hyperon pole term. The latter mechanism has been ignored in all previous calculations [20, 23–25] that relied on the very forward K^+ angular LEPS data [15, 16], where its contribution was expected to be small.

We have shown that when the contributions from the $N^*(2120)$ resonance and the $\Lambda(1115)$ are taken into account, both the new CLAS and the previous LEPS data can be simultaneously described. Actually, we find an overall good description of the data, both at forward and at backward K^+ angles, and for the whole range of measured γp invariant masses. The contribution of the u−channel $\Lambda(1115)$ pole term produces an enhancement at backward angles, and it becomes more and more rele-

vant as the photon energy increases, becoming essential above $W \geq 2.35$ GeV and $\cos\theta_{c.m.} \leq -0.5$. On the other hand, the CLAS data (see for instance Fig. 6), clearly support the existence of an odd parity 3/2 wide nucleon resonance with a mass in the region of 2.1 GeV, a width of around 200 MeV and a large partial decay width into Λ^*K. The recent analysis carried out in [30] of $\Lambda(1520)$ electroproduction off the proton also concludes that the D_{13} $N^*(2120)$ resonance plays an important role. It is re-assuring that the N^* couplings used in [30] turn out to be quite similar to those determined in this work. These characteristics could be easily accommodated within the constituent quark model results of Capstick and Roberts in Ref. [29]. Such resonance might be identified with the two stars PDG $N^*(2120)$ state. This would confirm previous claims [24, 25] from the analysis of the bump structure in the LEPS differential cross section at forward K^+ angles discussed in Fig. 4, and contradict previous negative claims made in [21] and [27] regarding this point.

Following [29], besides the $N^*(2120)$ D_{13} resonance, both of the weakly established states $N(2090)$ S_{11} and $N(2200)$ D_{15} [in the 2012 PDG review [2], these excited nucleons appear in the listings as the two-star $N(1895)$ and $N(2060)$, respectively], were also visible in $\Lambda(1520)K$ production reactions [see Fig. 6 of Ref. [29]]. If these resonances were take into account, one might wonder whether their contributions could affect the $N^*(2120)$ parameters in a significant way. Fortunately, the work of S. Nam on electroproduction of $\Lambda(1520)$ off the nucleon [30] sheds some light into this issue. There, the $D_{13}(2120)$, $S_{11}(2090)$ and $D_{15}(2200)$ resonances were considered, and it was found that the contributions of the two latter ones are negligible and much smaller than that of the $D_{13}(2120)$ state [see Figs. 6(a) and 11(a) in Ref. [30]].

On the other hand, the N^* resonance parameters from the new fits carried out in this work turn out to be in reasonable agreement with those obtained in Ref. [24], and the bulk of the conclusions of that reference still hold. In particular, the sign discrepancy (see Fig. 6 in [24]) of the predictions of the model for the polar-angle average photon-beam asymmetry, as a function of E_γ, with the SPring-8 LEPS data of Ref. [16] still persists.

In summary, we conclude that the associated strangeness production reaction $\gamma p \to K^+\Lambda(1520)$ is an adequate tool to study the properties of the $N^*(2120)$ resonance, and provides strong hints of its existence. This would corroborate the theoretical expectations of the chiral inspired unitary [4, 6] and constituent quark [29] models, and would make more plausible the analysis of the $\gamma p \to K^0\Sigma^+$ CBELSA/TAPS data carried out in [32], where the existence of a $J^P = 3/2^-$ nucleon excited state around 2 GeV has also been claimed. In addition, the study of the $\gamma p \to K^+\Lambda(1520)$ reaction also sheds light on the structure of $\Lambda(1520)$ [4, 49], and its properties such as the $\bar{K}^*N\Lambda^*$ [23] and $K\Lambda^*N^*$ vertices (this work and Ref. [24]) and its radiative $\Lambda^* \to \Lambda\gamma$ decay [h_1 and h_2 magnetic couplings, Eq. (4), determined in this work].

Acknowledgments

[1] E. Klempt and J. M. Richard, Rev. Mod. Phys. **82**, 1095 (2010).
[2] J. Beringer et al., [Particle Data Group], Phys. Rev. D **86**, 010001 (2012).
[3] S. Capstick and W. Robert, Prog. Part. Nucl. Phys. **45**, S241 (2000), and references therein.
[4] D. Gamermann, C. Garcia-Recio, J. Nieves and L. L. Salcedo, Phys. Rev. D **84**, 056017 (2011).
[5] S. Sarkar, B. -X. Sun, E. Oset and M. J. Vicente Vacas, Eur. Phys. J. A **44**, 431 (2010).
[6] E. Oset and A. Ramos, Eur. Phys. J. A **44**, 445 (2010).
[7] M. Pavon Valderrama, J. -J. Xie and J. Nieves, Phys. Rev. D **85**, 017502 (2012).
[8] B. -X. Sun, H. -X. Chen and E. Oset, Eur. Phys. J. A **47**, 127 (2011).
[9] B. S. Zou, eConf C **070910**, 112 (2007), and references therein.
[10] N. Mistry, S. Mori, D. Sober, and A. Sadoff, Phys. Lett. B **24**, 528 (1967).
[11] W. Blanpied, J. Greenberg, V. Hughes, P. Kitching, and D. Lu, Phys. Rev. Lett. **14**, 741 (1965).
[12] A. M. Boyarski et al., Phys. Lett. B **34**, 547 (1971).
[13] D. P. Barber et al. (LAMP2 Collaboration), Z. Phys. C **7**, 17 (1980).
[14] S. P. Barrow *et al.* [CLAS Collaboration], Phys. Rev. C **64**, 044601 (2001).
[15] N. Muramatsu et al. (LEPS Collaboration), Phys. Rev. Lett. **103**, 012001 (2009).
[16] H. Kohri et al. (LEPS Collaboration), Phys. Rev. Lett. **104**, 172001 (2010).
[17] F. W. Wieland, J. Barth, K. H. Glander, J. Hannappel, N. Jopen, F. Klein, E. Klempt and R. Lawall *et al.*, Eur. Phys. J. A **47**, 47 (2011) [Erratum-ibid. A **47**, 133 (2011)].
[18] K. Moriya *et al.* [CLAS Collaboration], Phys. Rev. C **88**, 045201 (2013).
[19] S. I. Nam, A. Hosaka, and H.-C. Kim, Phys. Lett. B **579**, 43 (2004); Phys. Rev. D **71**, 114012 (2005): Phys. Lett. B **633**, 483 (2006); J. Korean Phys. Soc. **49**, 1928 (2006).
[20] S.-I. Nam, A. Hoska, and H.-C. Kim, Phys. Rev. **D71**, 114012 (2010).
[21] S. I. Nam, Phys. Rev. C **81**, 015201 (2010).
[22] A. I. Titov, B. Kämpfer, S. Datá, and Y. Ohashi, Phys. Rev. C **72**, 035206 (2005); ibid **C 74**, 055206 (2006).
[23] H. Toki, C. García-Recio, and J. Nieves, Phys. Rev. D **77**, 034001 (2008).
[24] Ju-Jun Xie, and J. Nieves, Phys. Rev. **C 82**, 045205 (2010).
[25] J. He and X. R. Chen, Phys. Rev. C **86**, 035204 (2012).
[26] C. Garcia-Recio, J. Nieves and L. L. Salcedo, Phys. Rev. D **74**, 034025 (2006).
[27] S. I. Nam and C. W. Kao, Phys. Rev. C **81**, 055206 (2010).
[28] A. V. Anisovich, R. Beck, E. Klempt, V. A. Nikonov, A. V. Sarantsev and U. Thoma, Eur. Phys. J. A **48**, 15 (2012).
[29] S. Capstick, and W. Roberts, Phys. Rev. D **58**, 074011 (1998).
[30] S. I. Nam, J. Phys. G **40**, 115001 (2013).
[31] Ju-Jun Xie, and Bo-Chao Liu, Phys. Rev. C (**87**), 045210 (2013).
[32] A. Ramos and E. Oset, Phys. Lett. B **727**, 287 (2013).
[33] R. Ewald, B. Bantes, O. Bartholomy, D. Bayadilov, R. Beck, Y. A. Beloglazov, K. T. Brinkmann and V. Crede et al., Phys. Lett. B 713, 180 (2012).
[34] J. J. Swart, Rev. Mod. Phys. **35**, 916 (1963); *Erratum-ibid*, **37**, 326 (1965).
[35] A. Reuber, K. Holinde and J. Speth, Nucl. Phys. A **570**, 543 (1994).
[36] A. Pich, Rep. Prog. Phys. **58**, 563 (1995).
[37] S. Scherer and M. R. Schindler, Lect. Notes Phys. **830**, pp.1 (2012).
[38] T. S. Mast, M. Alston-Garnjost, R. O. Bangerter, A. Barbaro-Galtieri, L. K. Gershwin, F. T. Solmitz and R. D. Tripp, Phys. Rev. Lett. **21**, 1715 (1968).
[39] J. W. Darewych, M. Horbatsch and R. Koniuk, Phys. Rev. D **28**, 1125 (1983).
[40] E. Kaxiras, E. J. Moniz and M. Soyeur, Phys. Rev. D **32**, 695 (1985).
[41] M. Warns, W. Pfeil and H. Rollnik, Phys. Lett. B **258**, 431 (1991).
[42] Y. Umino and F. Myhrer, Nucl. Phys. A **529**, 713 (1991).
[43] R. Bijker, F. Iachello and A. Leviatan, Annals Phys. **284**, 89 (2000)
[44] T. Van Cauteren, J. Ryckebusch, B. Metsch and H. -R. Petry, Eur. Phys. J. A **26**, 339 (2005)
[45] L. Yu, X. -L. Chen, W. -Z. Deng and S. -L. Zhu, Phys. Rev. D **73**, 114001 (2006).
[46] M. Doring, E. Oset and S. Sarkar, Phys. Rev. C **74**, 065204 (2006)
[47] N. Awaji et al., *Energy Dependent Partial Wave Analysis On Single Pion Photoproduction*, Bonn, West Germany, Proceedings of the 10th International Symposium on Lepton and Photon Interactions at High Energy.
[48] C. Amsler *et al.* [Particle Data Group Collaboration], Phys. Lett. B **667**, 1 (2008).
[49] L. Roca, S. Sarkar, V. K. Magas and E. Oset, Phys. Rev. C **73**, 045208 (2006).